Supporting Information

Rhodamine 6G and phloxine B as photosensitizers for inkjet-printed indium oxide phototransistors

Liam Gillan [a)], Fei Liu [a)], Sanna Aikio[b)], Jaakko Leppäniemi [a)]*

a) VTT Technical Research Centre of Finland Ltd., Tietotie 3, Espoo, 02150, Finland

b) VTT Technical Research Centre of Finland Ltd. Kaitoväylä 1, Oulu, 90590, Finland

[*]E-mail: liam.gillan@vtt.fi

Table S1. Properties of small molecule and polymer dyes identified as potential photosensitizing agents for In_2O_3 TFTs. Green colored font indicates possible suitability, whereas values in red colored font fall outside of the desired criteria of i) absorption peak close to 565 nm, ii) LUMO > -3.98 eV, iii) good solubility in inkjet-printable solvent.

Dye	Absorption peak (nm)	LUMO (eV)	Solvents	Solubility	Ref
Rhodamine 6G	530	-3.14	Ethanol	OK	[1,2]
Phloxine B	550	-2.64	Ethanol	OK	[3]
Rhodamine B	554	-3.2	Water/ ethanol	OK	[4-7]
poly(3-hexylthiophene-2,5-diyl) (P3HT)	560	-3.2	1,2-dichlorobenzene	OK	[8,9]
Pthalocyanine (CuPc)	652, 751	-3.1	Trichloromethane	Poor	[10-12]
Methylene blue	664	-	Water	OK	[5,13]
p-Phenylenediamine (PPD)	240, 303	-2.16	Water	OK	[14]
Thieno[3,4-b]-thiophene-co-benzodithiophene (PTB7)	550 to 750	-2.76	Chlorobenzene	OK	[15,16]
Cyanine dye (Cy7-T)	840	-4.2	-	-	[17]
Carbazoles	450	-3.19 to -2.73	-	-	[18]

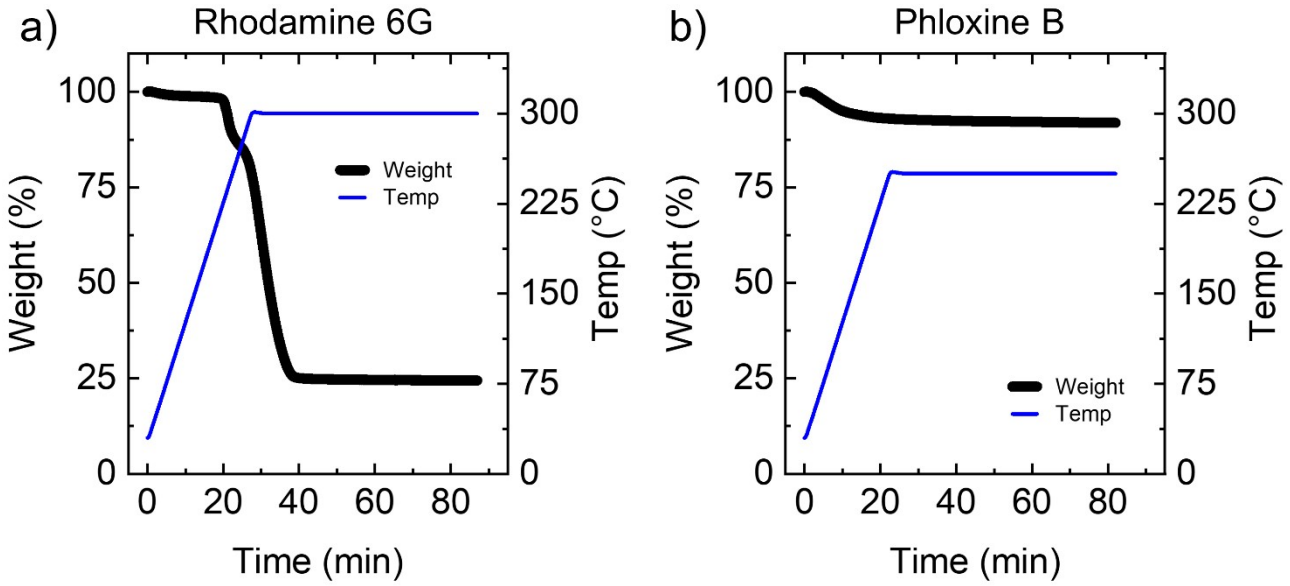

Figure S1. Thermal gravimetric analysis in N_2 at 10 °C/minute ramp rate up to 300 °C for rhodamine 6G (a), and 250 °C for phloxine B (b) at which point these temperatures were fixed for 60 minutes.

Table S2. Spin-coated samples for use in thin-film material characterization, showing constituent materials and sequential processing steps from left to right. For FTIR, the signal obtained from the sample in row one was used as a reference spectrum that was subtracted from FTIR spectra obtained from samples in rows two to seven. For fluorescence measurements (FL), bare glass substrate was used to generate a reference signal that was subtracted from all other FL measurements. OP denotes optical profilometry for surface roughness.

Materials and processing					**Use**
Glass	Plasma	In_2O_3 1.5 krpm (130°C, 15 min / 300°C, 30 min)	-	-	UV-Vis/FTIR/GIXRD
Glass	Plasma	In_2O_3 1.5 krpm (130°C, 15 min / 300°C, 30 min)	Plasma	InO_x 1.5 krpm (250°C, 15 min)	FTIR
Glass	Plasma	In_2O_3 1.5 krpm (130°C, 15 min / 300°C, 30 min)	Plasma	InO_x 1.5 krpm (300°C, 15 min)	FTIR
Glass	Plasma	In_2O_3 1.5 krpm (130°C, 15 min / 300°C, 30 min)	Plasma	PB 1.5 krpm (70°C, 15 min)	FTIR
Glass	Plasma	In_2O_3 1.5 krpm (130°C, 15 min / 300°C, 30 min)	Plasma	R6G 1.5 krpm (70°C, 15 min)	FTIR
Glass	Plasma	In_2O_3 1.5 krpm (130°C, 15 min / 300°C, 30 min)	Plasma	PB:InO_x 1.5 krpm (250°C, 15 min)	FTIR
Glass	Plasma	In_2O_3 1.5 krpm (130°C, 15 min / 300°C, 30 min)	Plasma	R6G:InO_x 1.5 krpm (300°C, 15 min)	FTIR
Glass	Plasma	PB 1.5 krpm (70°C, 15 min)	-	-	UV-Vis/FL/OP
Glass	Plasma	R6G 1.5 krpm (70°C, 15 min)	-	-	UV-Vis/FL/OP
Glass	Plasma	PB:InO_x 1.5 krpm (250°C, 15 min)	-	-	UV-Vis/GIXRD/FL/OP
Glass	Plasma	PB:InO_x 1.5 krpm (300°C, 15 min)	-	-	FL/OP
Glass	Plasma	R6G:InO_x 1.5 krpm (250°C, 15 min)	-	-	FL/OP
Glass	Plasma	R6G:InO_x 1.5 krpm (300°C, 15 min)	-	-	UV-Vis/GIXRD/FL/OP
Glass	Plasma	InO_x 1.5 krpm (250°C, 15 min)	-	-	XRD/FL/OP
Glass	Plasma	InO_x 1.5 krpm (300°C, 15 min)	-	-	XRD/FL/OP

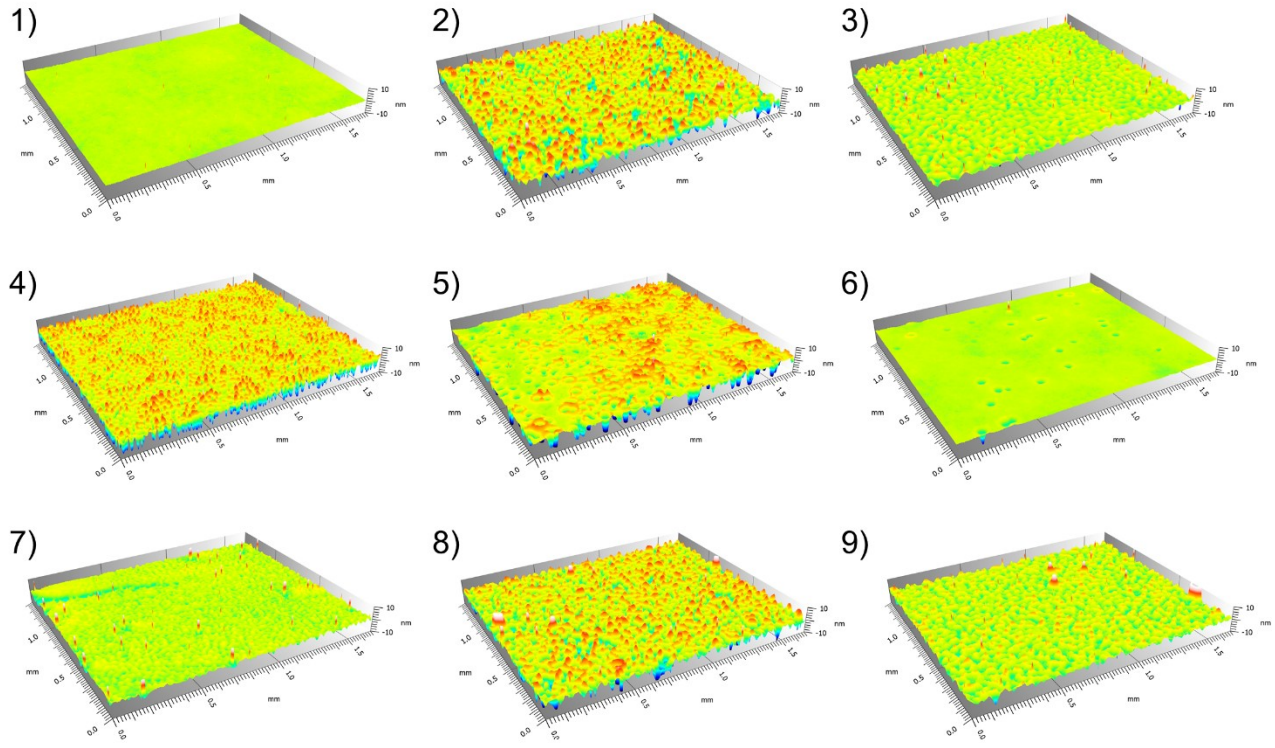

Sample number	Material	Surface roughness (nm)
1	Bare glass reference	0.0977
2	InO_x, 15 min 250 °C	1.5464
3	InO_x, 15 min 300 °C	0.5812
4	R6G, 15 min 70 °C	1.9688
5	R6G/InO_x, 15 min 250 °C	1.573
6	R6G/InO_x, 15 min 300 °C	0.141
7	PB, 15 min 70 °C	0.4485
8	PB/InO_x, 15 min 250 °C	1.5407
9	PB/InO_x, 15 min 300 °C	0.7542

Figure S2. Optical surface profilometry results presented both as 3D images and in tabulated form as arithmetical mean height (S_a-value in ISO 25178).

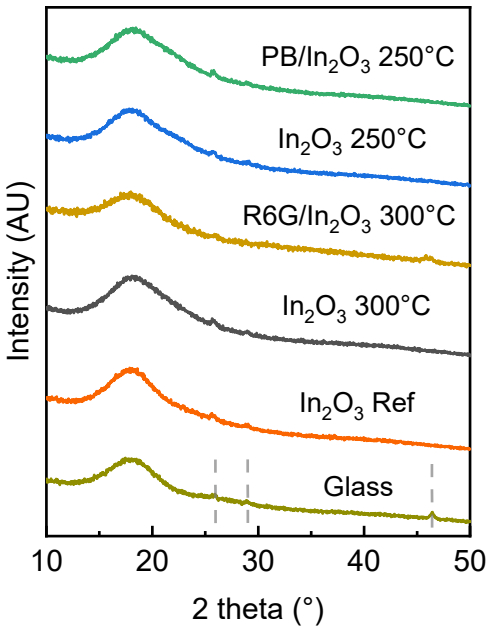

Figure S3. GIXRD spectra from a set of spin-coated oxide-based materials, depicting amorphous phase in all cases. Note that In_2O_3 Ref sample is 15 min 130 °C dried then 30 min 300 °C annealed, whereas In_2O_3 300 °C sample is only 15 min 300 °C annealed with no drying step. Glass is substrate in all cases.

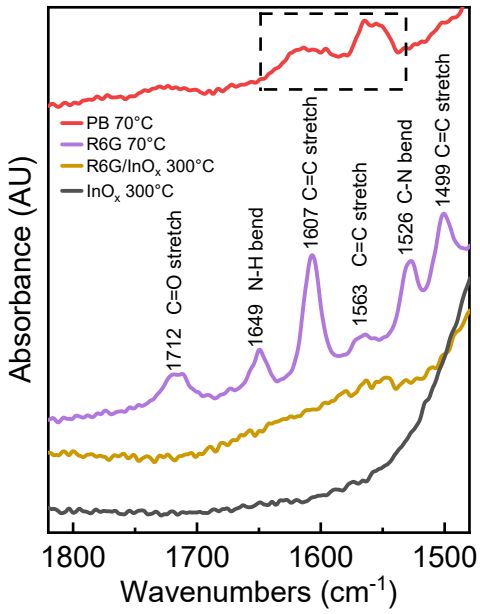

Figure S4. FTIR spectra of spin-coated films annotated with locations of major absorbance peaks for R6G [19,20]. The black dotted inset box encompasses the two major absorbance peaks observed for PB which are assigned to stretching vibrations of benzene, along with contribution from C=O stretching around 1600 cm^{-1} [21,22].

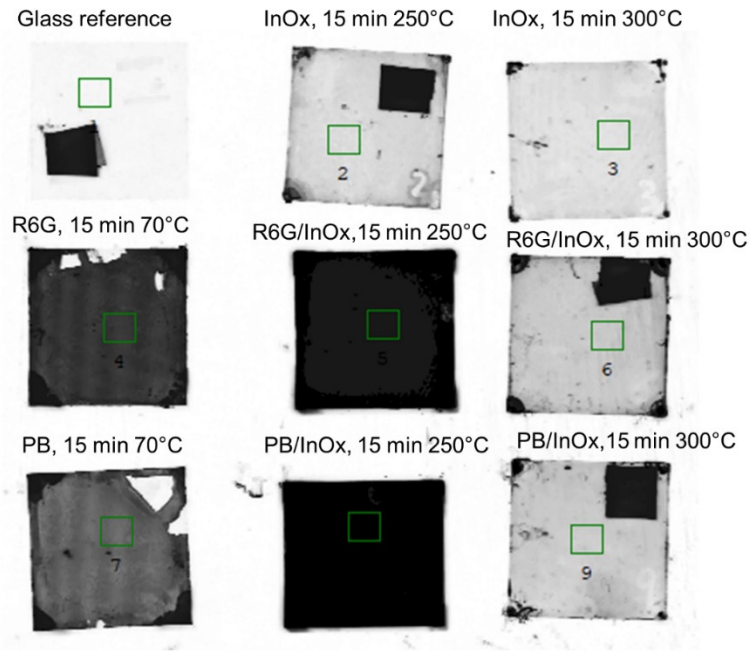

Figure S5. Image showing measured fluorescence intensities with an excitation wavelength of 532 nm and emission filter of 570 nm using non-linear inverted grey scale where darker color represents higher fluorescence intensity. Fluorescence intensity values of each sample (shown in Figure 3d) were calculated from an average value obtained within the green rectangle 4 mm wide and 3.6 mm high.

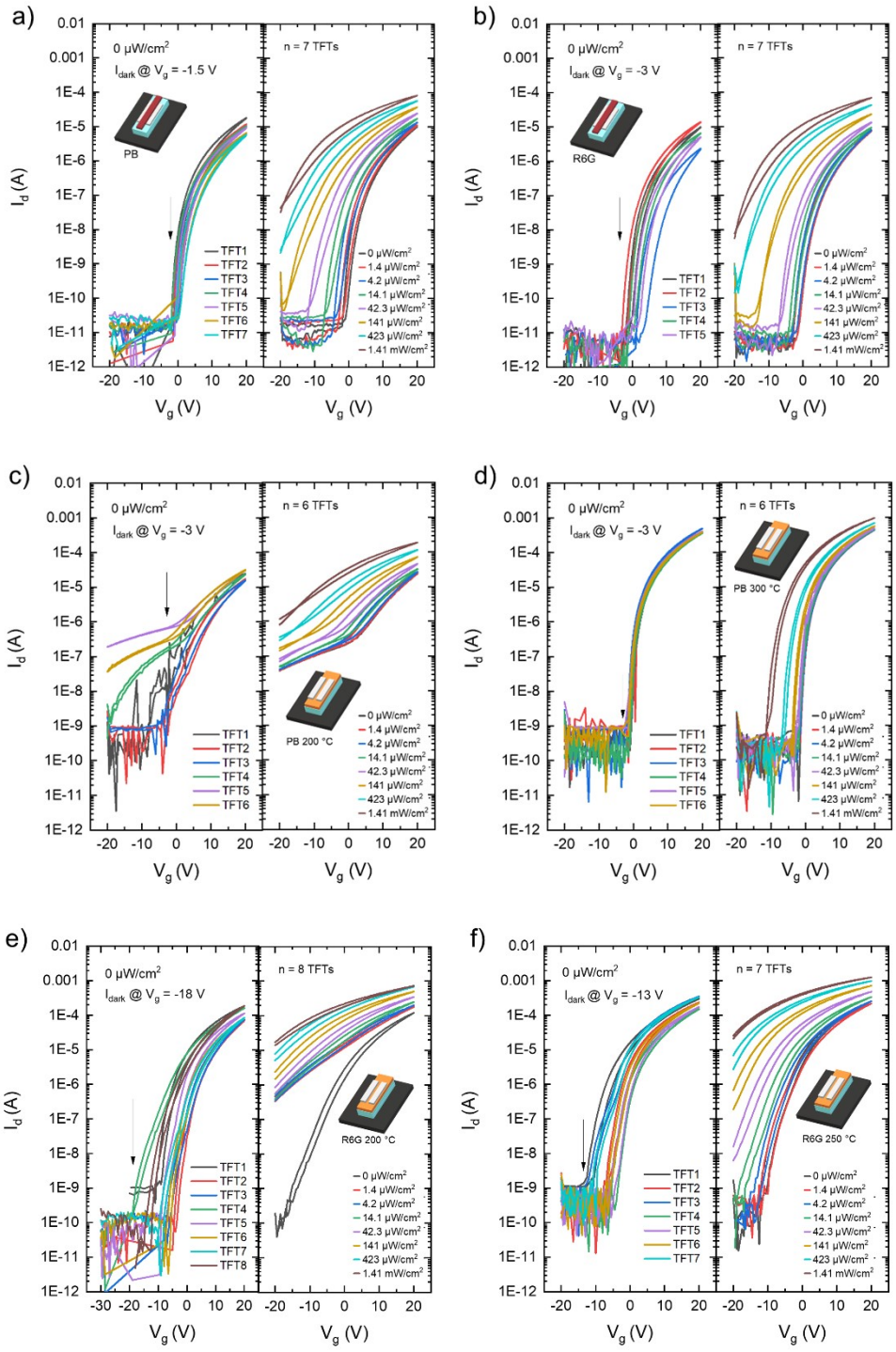

Figure S6. Dark condition transfer measurements of a series of In_2O_3 TFTs (left frames) with the dark current voltage listed for each device architecture being indicated by the vertical arrow, alongside average transfer measurements of the same series of In_2O_3 TFTs (right frames) in response to 565 nm light over a range of intensities for TFTs including a layer of a) phloxine B (PB), b) rhodamine 6G (R6G), c) PB/InOx treated at 200 °C, d) PB/InOx treated at 300 °C, e) R6G/InOx treated at 200 °C, and f) R6G/InOx layer treated at 250 °C.

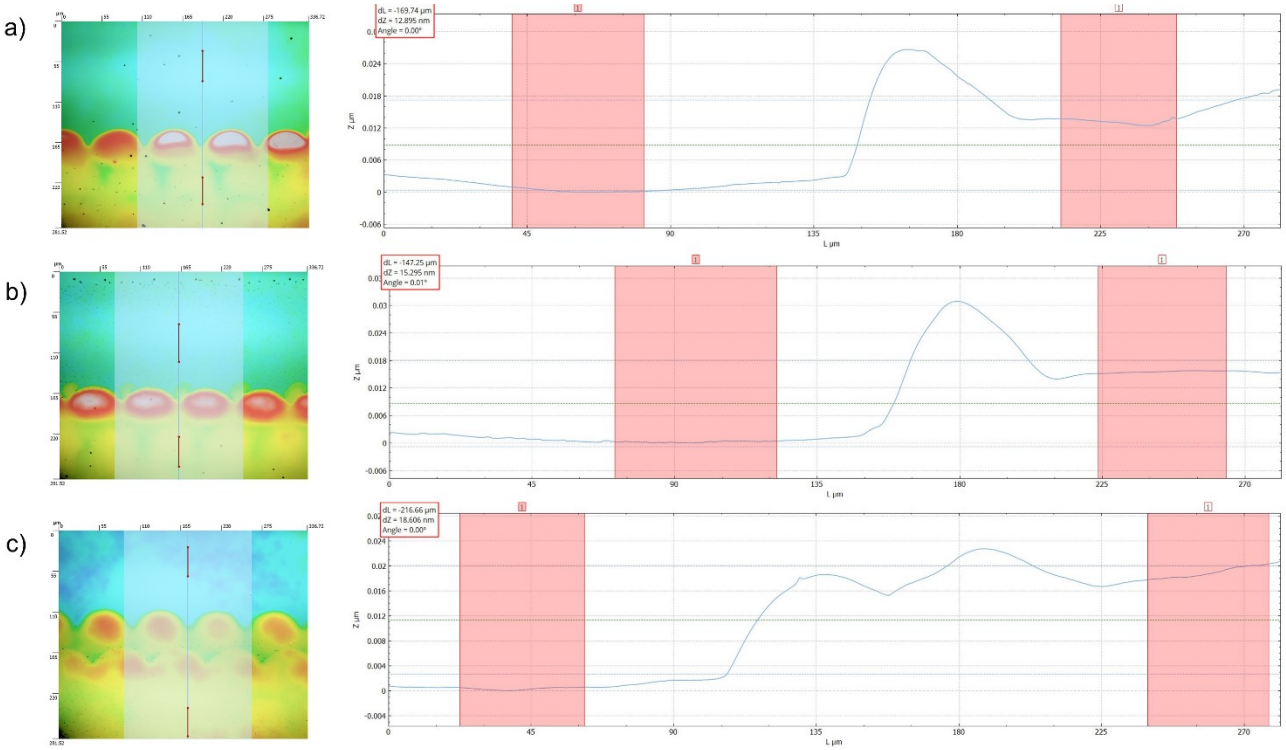

Figure S7. Optical profilometry top view (left) and side profile (right) for selected samples of (a) In_2O_3, (b) In_2O_3 plus R6G/InO_x, and In_2O_3 plus PB/InO_x as described in Table S3.

Table S3. Thickness data for inkjet-printed oxide films

Material	Sample name	Layer thickness (nm)	Average thickness (nm)	± std dev
2 layers In_2O_3	TFTE	12.895		
2 layers In_2O_3	TFTF	12.003		
2 layers In_2O_3	TFTG	13.827		
			12.908	0.745
2 layers In_2O_3 + 1 layer R6G/InO_x	TFTB	12.158		
2 layers In_2O_3 + 1 layer R6G/InO_x	TFTC	15.687		
2 layers In_2O_3 + 1 layer R6G/InO_x	TFTD	15.295		
			14.380	1.579
2 layers In_2O_3 + 1 layer PB/InO_x	TFTF	17.895		
2 layers In_2O_3 + 1 layer PB/InO_x	TFTG	17.399		
2 layers In_2O_3 + 1 layer PB/InO_x	TFTH	18.606		
			17.967	0.495

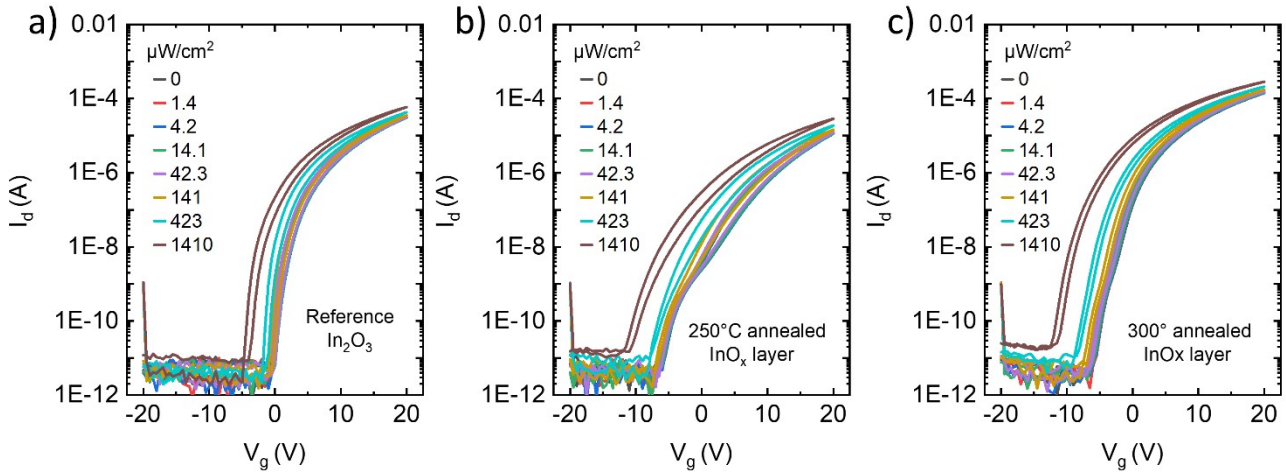

Figure S8. I/V curves measured across a range of illumination intensities for a) reference In_2O_3, b) In_2O_3 with an additional layer of InO_x annealed at 250 °C for 15 min, and c) In_2O_3 with an additional layer of InO_x annealed at 300 °C for 15 min.

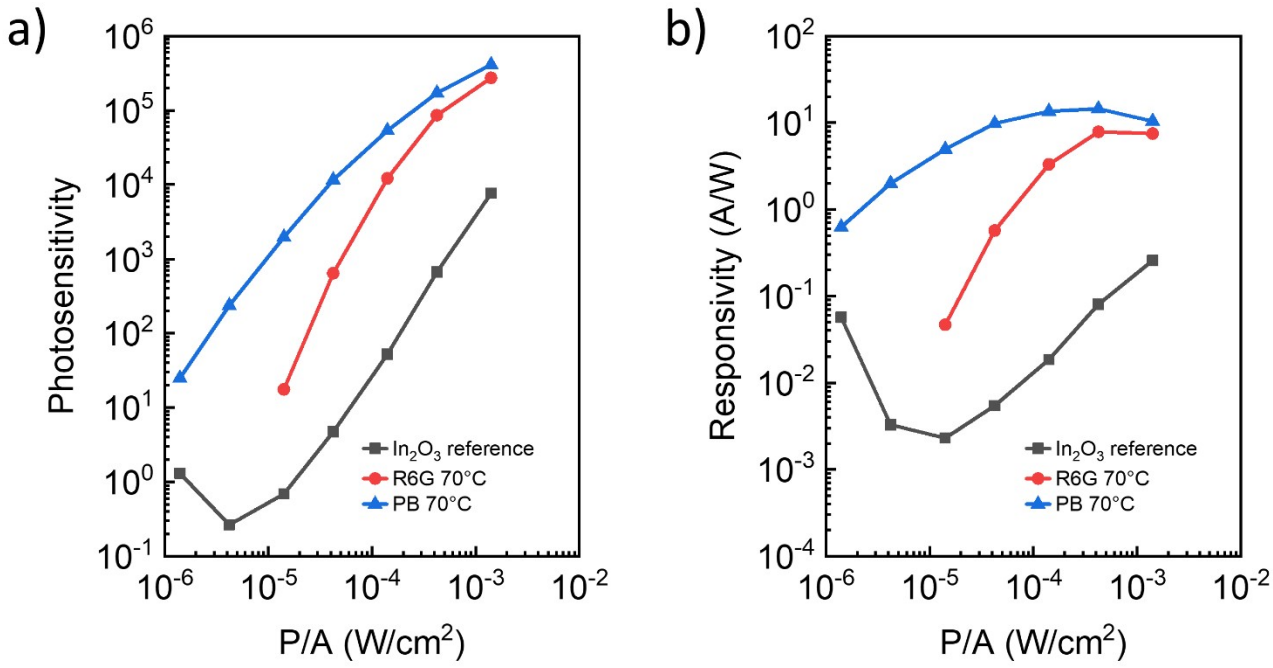

Figure S9. Optoelectronic figures of merit a) photosensitivity, and b) responsivity.

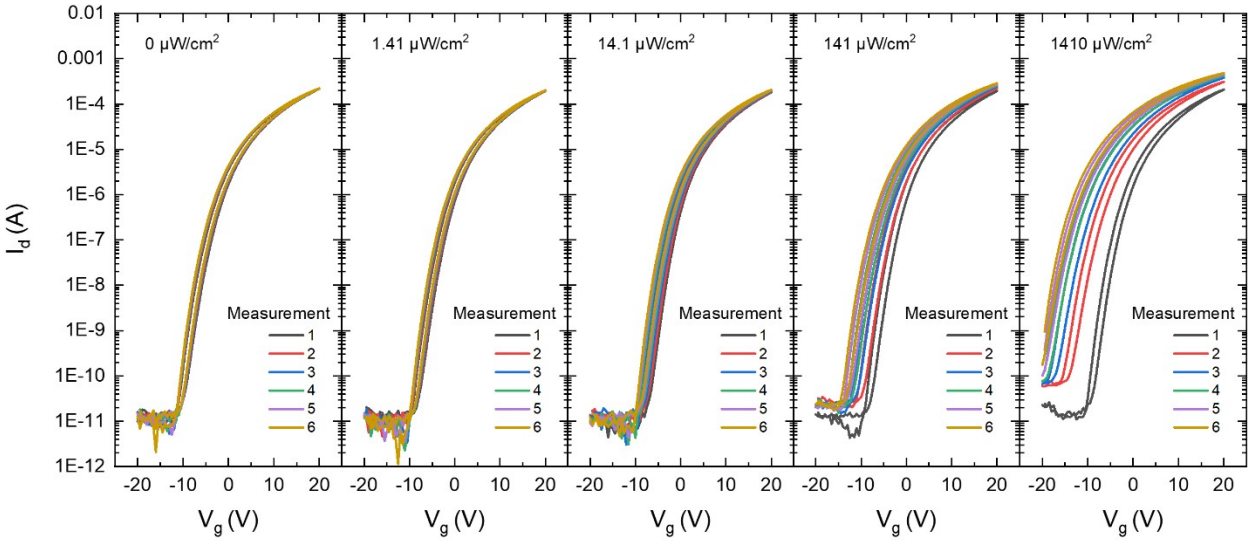

Figure S10. Six repeat I/V measurements from a R6G/InOx 300 °C device under each of 5 illumination conditions, with higher light intensities inducing a negative voltage shift. The first measurement of each illumination condition was performed in the dark.

References

[1] F. M. Zehentbauer, C. Moretto, R. Stephen, T. Thevar, J. R. Gilchrist, D. Pokrajac, K. L. Richard, and J. Kiefer, "Fluorescence spectroscopy of Rhodamine 6G: Concentration and solvent effects," *Spectrochim. Acta Part A Mol. Biomol. Spectrosc*., vol. 121, pp. 147–151, **2014**.

[2] S. H. Yu *et al.*, "Dye-Sensitized MoS2 Photodetector with Enhanced Spectral Photoresponse," *ACS Nano*, vol. 8, no. 8, pp. 8285–8291, Aug. **2014**.

[3] P. Ren, Y. Li, Y. Zhang, H. Wang, and Q. Wang, "Photoelectric Properties of DSSCs Sensitized by Phloxine B and Bromophenol Blue," *Int. J. Photoenergy*, vol. 2016, p. 11, **2016**.

[4] C. Teng, D. Xie, M. Sun, S. Chen, P. Yang, and Y. Sun, "Organic Dye-Sensitized CH3NH3PbI3 Hybrid Flexible Photodetector with Bulk Heterojunction Architectures," *ACS Appl. Mater. Interfaces*, vol. 8, no. 45, pp. 31289–31294, **2016**.

[5] J. Liu, G. Liu, W. Liu, and Y. Wang, "Turn-on fluorescence sensor for the detection of heparin based on rhodamine B-modified polyethyleneimine-graphene oxide complex," *Biosens. Bioelectron*., vol. 64, pp. 300–305, **2015**.

[6] M. S. Tehrani and R. Zare-Dorabei, "Highly efficient simultaneous ultrasonic-assisted adsorption of methylene blue and rhodamine B onto metal organic framework MIL-68(Al): central composite design optimization," *RSC Adv.*, vol. 6, no. 33, pp. 27416–27425, **2016**.

[7] I. S. Yahia, A. Jilani, M. M. Abutalib, S. Alfaify, M. Shkir, M. S. Abdel-wahab, A. A. Al-Ghamdi, and A. M. El-Naggar, "A study on linear and non-linear optical constants of Rhodamine B thin film deposited on FTO glass," *Phys. B*, vol. 490, pp. 25–30, **2016**.

[8] A. Yadav, A. Upadhyaya, S. K. Gupta, A. S. Verma, and C. M. S. Negi, "Poly-(3-hexylthiophene)/graphene composite based organic photodetectors: The influence of graphene insertion," *Thin Solid Films*, vol. 675, pp. 128–135, Apr. **2019**.

[9] C. Y. Kwong, W. C. H. Choy, A. B. Djurišić, P. C. Chui, K. W. Cheng, and W. K. Chan, "Poly(3-hexylthiophene): TiO2 nanocomposites for solar cell applications," *Nanotechnology*, vol. 15, no. 9, pp. 1156–1161, **2004**.

[10] C. Wang, X. Chen, F. Chen, and J. Shao, "Organic photodetectors based on copper phthalocyanine films prepared by a multiple drop casting method," *Org. Electron.*, vol. 66, pp. 183–187, **2019**.

[11] J. Li, F. Zhou, H. P. Lin, W. Q. Zhu, J. H. Zhang, X. Y. Jiang, and Z. L. Zhang, "Enhanced photosensitivity of InGaZnO-TFT with a CuPc light absorption layer," *Superlattices Microstruct.*, vol. 51, no. 4, pp. 538–543, **2012**.

[12] J. Pak, J. Jang, K. Cho, T. Y. Kim, J. K. Kim, Y. Song, W. K. Hong, M. Min, H. Lee, and T. Lee, "Enhancement of photodetection characteristics of MoS2 field effect transistors using surface treatment with copper phthalocyanine," *Nanoscale*, vol. 7, no. 44, pp. 18780–18788, **2015**.

[13] J. C. Dean, S. Rafiq, D. G. Oblinsky, E. Cassette, C. C. Jumper, and G. D. Scholes, "Broadband Transient Absorption and Two-Dimensional Electronic Spectroscopy of Methylene Blue," *J. Phys. Chem. A*, vol. 119, no. 34, pp. 9098–9108, **2015**.

[14] T. Chandrakalavathi, M. Reddeppa, T. Revathi, P. K. Basivi, S. K. Viswanath, G. Murali, M.-D. Kim, and R. Jeyalakshmi, "p-Pheneylendiamine functionalized rGO/Si heterostructure Schottky junction for UV photodetectors," *Diam. Relat. Mater.*, vol. 93, pp. 208–215, **2019**.

[15] P. H. Chang, Y. C. Tsai, S. W. Shen, S. Y. Liu, K. Y. Huang, C. S. Li, H. P. Chang, and C. I. Wu, "Highly Sensitive Graphene-Semiconducting Polymer Hybrid Photodetectors with Millisecond Response Time," *ACS Photonics*, vol. 4, no. 9, pp. 2335–2344, **2017**.

[16] Y. Liang, Z. Xu, J. Xia, S. T. Tsai, Y. Wu, G. Li, C. Ray, and L. Yu, "For the Bright Future-Bulk Heterojunction Polymer Solar Cells with Power Conversion Efficiency of 7.4%," *Adv. Mater.*, vol. 22, no. 20, pp. E135–E138, **2010**.

[17] H. Zhang, S. Jenatsch, J. De Jonghe, F. Nuësch, R. Steim, A. C. Véron, and R. Hany, "Transparent Organic Photodetector using a Near-Infrared absorbing Cyanine Dye," *Sci. Rep*., vol. 5, no. 9439, pp. 1–6, **2015**.

[18] S. El Mzioui, S. M. Bouzzine, M. Bourass, M. Naciri Bennani, and M. Hamidi, "A theoretical investigation of the optoelectronic performance of some new carbazole dyes," *J. Comput. Electron*., vol. 18, no. 3, pp. 951–961, **2019**.

[19] Y.-M. Zheng, R. F. Yunus, K. G. N. Nanayakkara, and J. P. Chen, "Electrochemical Decoloration of Synthetic Wastewater Containing Rhodamine 6G: Behaviors and Mechanism," *Ind. Eng. Chem. Res.*, vol. 51, no. 17, pp. 5953–5960, **2012**.

[20] H. Ren, D. D. Kulkarni, R. Kodiyath, W. Xu, I. Choi, and V. V. Tsukruk, "Competitive Adsorption of Dopamine and Rhodamine 6G on the Surface of Graphene Oxide," *ACS Appl. Mater. Interfaces*, vol. 6, no. 4, pp. 2459–2470, Feb. **2014**.

[21] J. R. Kim and S. Michielsen, "Photodynamic antifungal activities of nanostructured fabrics grafted with rose bengal and phloxine B against Aspergillus fumigatus," *J. Appl. Polym. Sci.*, vol. 132, no. 26, pp. 42114, **2015**.

[22] Y. Yin *et al.*, "A sodium alginate-based nano-pesticide delivery system for enhanced in vitro photostability and insecticidal efficacy of phloxine B," *Carbohydr. Polym.*, vol. 247, pp. 116677, **2020**.